

# Exploration of the Nature of Active Ti Species in Metallic Ti-Doped NaAlH<sub>4</sub>

Ping Wang,\* Xiang-Dong Kang, and Hui-Ming Cheng

Shenyang National Laboratory for Materials Science, Institute of Metal Research,  
Chinese Academy of Sciences, Shenyang 110016, China

Received: June 11, 2005; In Final Form: August 2, 2005

Clarification of the nature of active Ti species has been a key challenge in developing Ti-doped NaAlH<sub>4</sub> as a potential hydrogen storage medium. Previously, it has been greatly hindered by the invisibility of Ti-containing species in conventional analysis techniques. In the present study, for the first time, the catalytically active Ti-containing species have been definitely identified by X-ray diffraction in the hydrides doped with metallic Ti. It was found that mechanical milling of a NaH/Al mixture or NaAlH<sub>4</sub> with metallic Ti powder resulted in the formation of nanocrystalline Ti hydrides. The variation of the preparation conditions during the doping process leads to a slight composition variation of the Ti hydrides. The catalytic enhancement arising upon doping the hydride with commercial TiH<sub>2</sub> was quite similar to that achieved in the hydrides doped with metallic Ti. Moreover, the cycling stability that was previously established in metallic Ti-doped hydrides was also observed in the hydrides doped with TiH<sub>2</sub>. These results clearly demonstrate that the in situ formed Ti hydrides act as active species to catalyze the reversible dehydrogenation of NaAlH<sub>4</sub>. The mechanism by which Ti hydrides catalyze the reversible de-/hydrogenation reactions of NaAlH<sub>4</sub> was discussed.

## I. Introduction

Commercialization of fuel-cell-powered vehicles requires a safe and efficient hydrogen storage system to provide an onboard hydrogen source. However, decades of extensive efforts on traditional metal/alloy hydrides and nanostructured carbon materials have led to no viable system that can meet the stringent combined requirements on weight/volume energy density, operation conditions, reversibility, efficiency, and cost.<sup>1</sup> Recently, Bogdanović and Schwickardi have demonstrated that NaAlH<sub>4</sub> might undergo reversible de-/hydrogenation upon doping with a few mol % of Ti catalysts.<sup>2</sup> This finding offers a clear potential to achieve >5 wt % hydrogen storage at a moderate temperature condition and thus quickly stimulates worldwide interest in developing catalytically enhanced Ti–NaAlH<sub>4</sub> and other related light metal complex hydrides as practical hydrogen storage media.<sup>3–15</sup>

The hydrogen storage performance of the Ti–NaAlH<sub>4</sub> system at moderate temperature range is dominated by the catalytic enhancement arising upon doping with Ti catalyst. So far, however, the catalytic mechanism and even the nature of active Ti species have not been firmly established. There have been several different hypotheses proposed to picture the active Ti species in the doped hydrides. One is that the surface-localized species consisting of titanium metal or Al–Ti alloy acts as an active catalyst and is present in the hydride matrix in an X-ray amorphous form.<sup>2,5,16–23</sup> This hypothesis was partially supported by the observed H<sub>2</sub> evolution during the doping process, X-ray absorption and electron microscopy studies of the doped hydride at various states,<sup>2,5,16–22</sup> and also by theoretical calculation.<sup>23</sup> Alternatively, on the basis of the observation that lattice parameters of NaAlH<sub>4</sub> changed upon Ti doping, Sun et al. proposed that Ti cations with variable valence were incorporated into the host lattice and substituted for Na<sup>+</sup>.<sup>24,25</sup>

Recently, another possibility was suggested by Balema et al. that Ti hydride(s) might be formed during the doping or hydrogenation processes and contributed to the catalytic enhancement in the reversible de-/hydrogenation of NaAlH<sub>4</sub>.<sup>26</sup> While the formation of Ti hydride(s) from metallic Ti with the presence of hydrogen is thermodynamically favorable, the direct experimental evidence to support this speculation was rather limited.<sup>13</sup>

Quite recently, we found that metallic Ti powder could be directly utilized as a dopant precursor to prepare a catalytically enhanced Ti–NaAlH<sub>4</sub> system.<sup>27,28</sup> This novel process not only eliminates the problematic generation of byproducts and evolution of detrimental gas impurities in the traditional doping method, but also provides a new perspective to probe the puzzling nature of active Ti species. A systematic structure/property investigation along this new approach has provided convincing evidence of the nature of active Ti species in metallic Ti-doped NaAlH<sub>4</sub>.

## II. Experimental Section

The starting materials NaH (95%, 200 mesh), Al powder (99.95+%, –200 mesh), Ti powder (99.98%, –325 mesh), and TiH<sub>2</sub> (98%, 325 mesh) were all purchased from Sigma-Aldrich Corp. and used as received. Raw NaAlH<sub>4</sub> was purchased from Albemarle Corp. and purified following a procedure described in ref 27 before usage.

Mechanical milling, as a simple and effective preparation technique, has been generally adopted to prepare a variety of hydrogen storage materials with nanostructure, amorphous, or doped structures. The milling process is characterized by high-energy collision/grinding between grinding balls or between ball and container walls, which repeatedly induces fracturing and cold welding of sample particles. Fundamentals, application, and recent development of the milling technique can be found in general reviews<sup>29,30</sup> and books.<sup>31,32</sup>

\* Author to whom correspondence should be addressed. E-mail: pingwang@imr.ac.cn. Fax: +86 24 2389 1320.

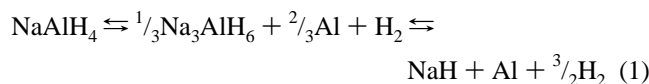
The mixtures of NaH + Al + Ti (1:1:0.04) and NaAlH<sub>4</sub> + Ti (1:0.04) were mechanically milled by using a Fritsch 7 Planetary mill at 400 rpm in a bowl, together with grinding balls made of stainless steel, respectively. The milling was performed under reactive H<sub>2</sub> or inert Ar atmosphere, with an initial pressure of about 0.8 and 0.1 MPa, respectively. The ball-to-powder ratio was about 40:1. To check the catalytic effect of TiH<sub>2</sub>, the mixtures of NaH + Al + TiH<sub>2</sub> (1:1:0.04) and NaAlH<sub>4</sub> + TiH<sub>2</sub> (1:0.04) were also mechanically milled under identical conditions to that applied for metallic Ti doping. In addition, to further check the phase transformation of the NaH/Ti mixture during the milling process, the mixture in a molar ratio of 2:1 was mechanically milled under Ar atmosphere for 2 h. All the sample operations were performed in an Ar-filled glovebox, in which the H<sub>2</sub>O/O<sub>2</sub> levels were below 1 ppm.

Hydriding/dehydriding performances of as-prepared samples were examined by using a carefully calibrated Sievert's type apparatus. The leakage rate of the system in a pressure holding test (12 MPa hydrogen and 120 h) was lower than  $1.0 \times 10^{-7}$  mol/h. The mass of the sample for every measurement run was typically around 300 mg. Precise pressure measurement and temperature control were accomplished by using a high-precision pressure transducer and silicon oil bath, respectively. A typical cyclic experiment entailed dehydrogenation at 150 °C and rehydrogenation at 120 °C with an initial pressure condition of <1 Torr and ~10 MPa, respectively. The high-purity hydrogen gas (with a purity of 99.999%) was further purified by using a hydrogen storage alloy system. To allow a practical evaluation of hydrogen storage performance, all the components were taken into account in the determination of the hydrogen capacity.

The samples were characterized by powder X-ray diffraction (XRD, Rigaku D/MAX-2500, Cu K $\alpha$  radiation,  $\lambda = 1.54056$  Å) and scanning electron microscopy (SEM, LEO Supra 35 and JSM 6301F) equipped with an energy-dispersive X-ray (EDX) analysis unit (Oxford). All the sample preparation was performed in the glovebox. To minimize the H<sub>2</sub>O/O<sub>2</sub> contamination during the XRD examination, a small amount of grease was used to cover the surface of the samples. The SEM samples were prepared by spreading the dry powders on conducting tape supported on a copper pole. The subsequent sample transfer into the SEM equipment was performed in a specially designed Ar-filled device.

### III. Experimental Results

Ti-doped NaAlH<sub>4</sub> can be prepared from either the hydrogenated state NaAlH<sub>4</sub> or the dehydrogenated state NaH/Al mixture according to eq 1.



In a systematic investigation, metallic Ti-doped hydrides have been mechanically prepared from different starting materials and under different milling atmospheres, reactive H<sub>2</sub> or inert Ar. Figure 1 gives the XRD patterns of the materials that were prepared under varied conditions. It was found that the various doping processes all resulted in the formation of Ti hydrides, but the composition of which may vary upon changing the doping conditions. As shown in Figure 1a, TiH<sub>2</sub> was formed during the process of mechanical milling of the NaH/Al mixture with Ti powder under Ar atmosphere. The detected peaks at  $2\theta = 35.2, 40.86, 59.25,$  and  $70.84^\circ$  can be assigned to the (111), (200), (220), and (311) diffraction of the tetragonal TiH<sub>2</sub> phase, respectively (according to JCPDS 03-0859). Additionally,

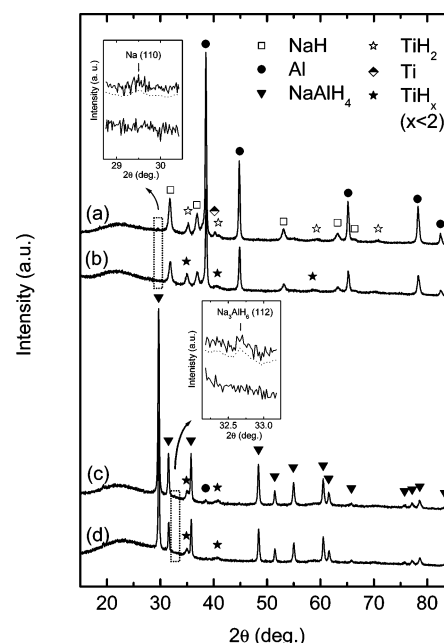
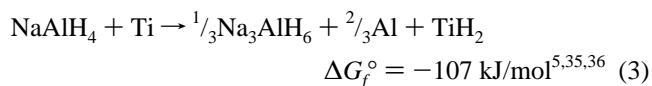


**Figure 1.** XRD patterns of the samples that were prepared under varied conditions. (a) NaH + Al + 4 mol % Ti milled under Ar atmosphere for 10 h; (b) NaH + Al + 4 mol % Ti milled under H<sub>2</sub> atmosphere for 10 h; (c) NaAlH<sub>4</sub> + 4 mol % Ti milled under Ar atmosphere for 10 h; (d) NaAlH<sub>4</sub> + 4 mol % Ti milled under H<sub>2</sub> atmosphere for 10 h. The inserted figures give the magnified patterns of the framed parts (and corresponding smoothed lines) in Figure 1.

the (101) diffraction of metallic Ti with the highest relative intensity was still detected even after 10 h of milling. However, after an identical milling period of 10 h, metallic Ti was not detectable after changing the milling atmosphere from Ar to H<sub>2</sub> and/or varying the starting material from NaH/Al mixture to NaAlH<sub>4</sub>. More interestingly, as seen in patterns (b), (c), and (d), the change of the above-mentioned milling conditions also results in the variation of Ti hydride from tetragonal TiH<sub>2</sub> to nonstoichiometric cubic Ti hydride(s). Here it should be noted that the definite identification of the actual composition of the nonstoichiometric Ti hydride phase is difficult, owing to the relatively weak and widened diffraction peaks as well as a continuous composition range of the cubic phase.<sup>26,33</sup> The nonstoichiometric Ti hydride(s) were denoted as TiH<sub>x</sub> ( $x < 2$ ). In all cases, the formed Ti hydrides are nanocrystalline. According to the Scherrer equation, the grain sizes of Ti hydrides in the samples milled for 10 h are around 10 nm.

The formation of nanocrystalline Ti hydride(s) under varied doping conditions involves different reaction pathways, as follows. For simplicity, the slight composition variation of the Ti hydrides is ignored. Other than when specified, all the formed Ti hydrides are generalized as TiH<sub>2</sub> or Ti hydride hereinafter.



When the metallic Ti doping was performed under Ar atmosphere, Ti hydrides should be formed via reactions 2 and 3 because NaH and NaAlH<sub>4</sub> provide the sole H source, respectively. This was confirmed in our careful examination of the XRD patterns (a) and (c). As seen in the inserted figures in

Figure 1, the mechanically milled NaH/Al mixture or NaAlH<sub>4</sub> with 4 mol % Ti powder under Ar atmosphere resulted in the formation of a small amount of metallic Na and Na<sub>3</sub>AlH<sub>6</sub>, respectively. The reduction of NaH by metallic Ti was further evidenced by the clear detection of metallic Na in our XRD examination of the mechanically milled NaH/Ti mixture in a 2:1 molar ratio under Ar atmosphere (results not shown here). In the latter case, the detection of Na<sub>3</sub>AlH<sub>6</sub> was consistent with that of Al (at  $2\theta = 38.5^\circ$ ) in pattern (c). While for the samples milled under H<sub>2</sub> atmosphere, no new phase other than Ti hydride(s) can be detected. Therefore, the metallic Ti reacts directly with the atmospheric H<sub>2</sub> according to eq 4. This solid–gas reaction is quite understandable in view of the well-known surface catalysis function of Ti in dissociative H chemisorption, where electron transferring from Ti to H<sub>2</sub> favors H–H bond dissociation by occupying an H–H antibonding orbital.<sup>37</sup> Also, it was supported by the thermochemical consideration, especially after taking into account the increased free-energy change due to the application of 0.8 MPa hydrogen during the doping process.

$$\Delta G_f = \Delta G_f^\circ - R \cdot T \cdot \ln(P_{H_2}/P^\circ) = -110.2 \text{ kJ/mol}$$

In addition, the instant temperature and pressure conditions created by collision between vial wall and balls and/or among the balls during the milling process may further favor the in situ hydrogenation of Ti. On the other hand, the lower thermodynamic driving force of the NaH/Ti solid-state reaction (eq 2), in comparison with those of the other reaction pathways, may account for the observed incomplete hydrogenation of metallic Ti during the doping process. Here, it should be noted that the process of Ti alloying with Al is also thermodynamically favorable. But in our XRD examination, no Al–Ti alloy could be definitely identified.

In the samples mechanically doped with metallic Ti, Ti hydrides have been identified as the sole newly formed Ti-containing species in the XRD examination. Moreover, in most cases, the metallic Ti was largely consumed. These results clearly suggest a possible correlation between the formed Ti hydride(s) and catalytic enhancement achieved in Ti-doped NaAlH<sub>4</sub>.

To check this possibility, TiH<sub>2</sub> was directly utilized as the dopant precursor and mechanically milled with NaH/Al mixture and NaAlH<sub>4</sub>, respectively. Before being subjected to mechanical doping, the commercial Ti hydride was examined by XRD, the actual composition of which was identified as TiH<sub>1.924</sub>. Figure 2 gives a typical comparison on the dehydrogenating/rehydrogenating performance between the NaH/Al mixtures doped with Ti hydride and metallic Ti powder, respectively. It was found that these two materials exhibited similar hydrogen storage performances. More exactly, the dehydrogenating/rehydrogenating rates and hydrogen capacity of the TiH<sub>2</sub>-doped sample were even slightly higher than those achieved in metallic Ti-doped hydride. Similar phenomenon was also observed in our examination of the samples doped from NaAlH<sub>4</sub>. Currently, the mechanism involved is not clear.

Further investigation found that the catalytic enhancement arising upon doping the hydrides with Ti hydride persisted in the following dehydrogenating/rehydrogenating cycles. Moreover, the cycling performances of the TiH<sub>2</sub>-doped hydrides were quite similar to those observed in the samples doped with metallic Ti. Figure 3a gives the dehydrogenating profiles at the first 4 cycles of the sample prepared by mechanically milling the NaH/Al mixture with 4 mol % TiH<sub>2</sub> under Ar atmosphere for 10 h. For comparison purposes, the cycling profiles of the metallic Ti-

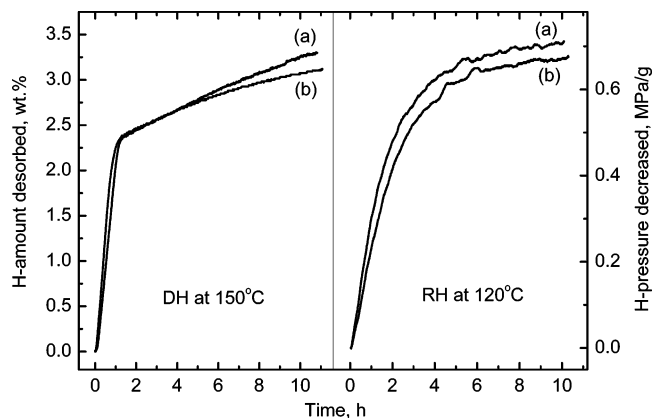


**Figure 2.** Typical comparison on the dehydrogenating (DH)/rehydrogenating (RH) profiles between the samples that were prepared by mechanically milling NaH/Al with (a) 4 mol % TiH<sub>2</sub>, (b) 4 mol % metallic Ti under Ar atmosphere for 10 h.

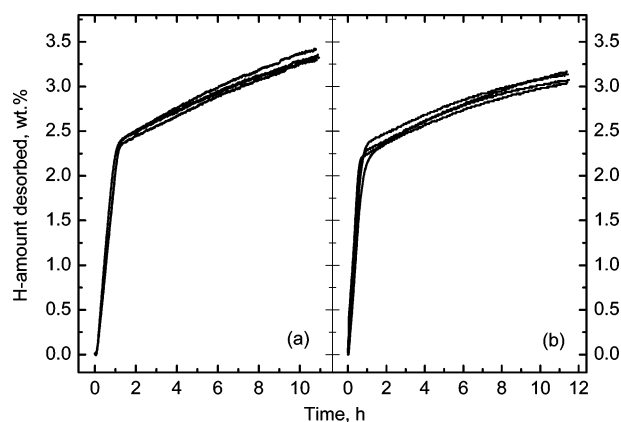


**Figure 3.** Dehydrogenating profiles (150 °C) at the first 4 cycles of the samples prepared by mechanically milling NaH/Al with (a) 4 mol % TiH<sub>2</sub>, (b) 4 mol % metallic Ti under Ar atmosphere for 10 h.

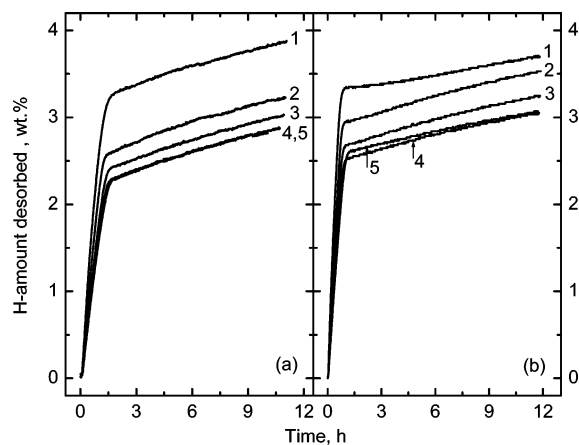


**Figure 4.** Dehydrogenating profiles (150 °C) at the first 5 cycles of the samples prepared by mechanically milling NaAlH<sub>4</sub> with (a) 4 mol % TiH<sub>2</sub>, (b) 4 mol % metallic Ti under Ar atmosphere for 10 h.

doped sample prepared under identical conditions were included in Figure 3b. In both materials, the dehydrogenating rate and the hydrogen capacity were well maintained in the dehydrogenating/rehydrogenating cycles. Figure 4a and b give the cycling performances of the NaAlH<sub>4</sub> samples doped with TiH<sub>2</sub> and metallic Ti, respectively. The H capacity of both materials underwent serious degradation during the first 4 cycles and then stabilized at about 3 wt %. Meanwhile, the dehydrogenating kinetics was well maintained in both samples. Here, it was noticed that the capacity loss mainly came from the decreased H capacity



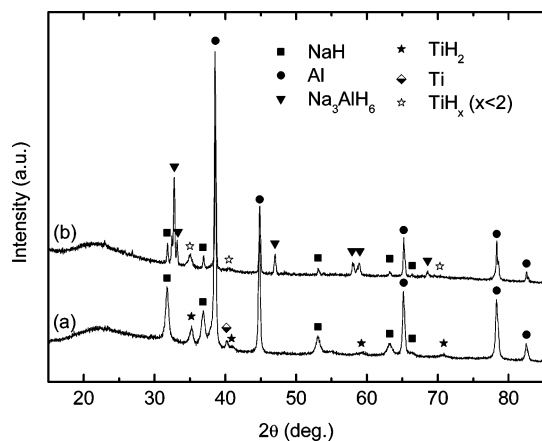


**Figure 5.** XRD patterns of the sample that was prepared by mechanically milling NaH/Al with 4 mol % metallic Ti under Ar atmosphere for 10 h (a) as-milled, (b) after 3 cycles in dehydrogenated state.

available from the  $\text{NaAlH}_4/\text{Na}_3\text{AlH}_6 + \text{Al}$  dehydriding step, indicating the incomplete rehydrogenation of  $\text{Na}_3\text{AlH}_6$  during the rehydriding process. This was confirmed by XRD examination (the results not shown here). In addition, these results also suggest that the observed difference on dehydriding performance between the samples doped from NaH/Al and  $\text{NaAlH}_4$ , respectively, should be attributed to the change of the starting materials, but not the slight composition variation of the formed Ti hydrides. In this regard, further investigation is still required to get a better understanding of the local phase distribution and the nucleation-growth mechanisms involved in the repeated decomposition/reconstruction of tetra- and hexahydrides.

The phase structure of the metallic Ti-doped hydrides at various stages was further examined by XRD. Figure 5 gives the XRD patterns of the as-milled sample and that after three cycles in the dehydrogenated state. After three cycles, the remaining metallic Ti after mechanical milling could no longer be detected, indicating the hydrogenation of metallic Ti during the cycles. Interestingly, it was also observed that the tetragonal  $\text{TiH}_2$  initially formed during the doping process had transformed to nonstoichiometric cubic  $\text{TiH}_x$  ( $x < 2$ ) during the dehydriding/rehydriding cycles. However, according to the cycling performance (as seen in Figure 3), such a slight compositional variation and tetragonal–cubic transition of the Ti hydride phase seems to produce no significant influence on the hydrogen storage properties of the doped hydrides.

The combined phase characterization and property measurements strongly suggest that the in situ formed Ti hydride(s) during the doping process acts as a active species and contributes to the catalytic enhancement in metallic Ti-doped  $\text{NaAlH}_4$ .

A prominent feature of the metallic Ti-doped hydrides is that the hydrogen storage performance of the materials is highly dependent on the milling time.<sup>27,28</sup> A systematic phase/structure investigation shows that such property-milling time dependence should be understood from the combined effects of the following three aspects:

(1) Increased catalyst amount. Figure 6 presents the XRD patterns of NaH + Al + 4 mol % Ti powder mixtures mechanically milled for a period ranging from 1 to 10 h. Judging from the augmented diffraction intensity, the amount of the formed  $\text{TiH}_2$  phase increases with increasing the milling time.

(2) Decreased particle size of the doped materials. As shown in Figure 7, with increasing the milling time from 1 to 10 h, the average particle size of the mechanically prepared sample has been reduced from around 30–40  $\mu\text{m}$  to less than 10  $\mu\text{m}$ .

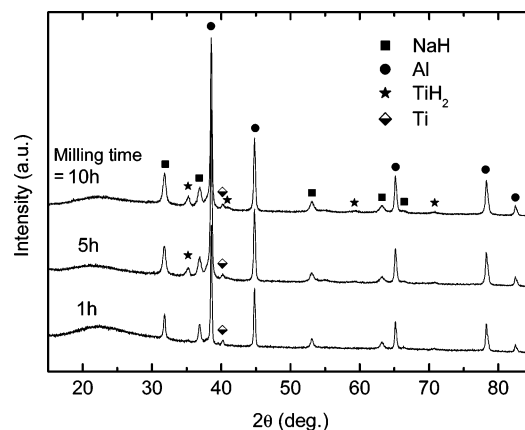


**Figure 6.** XRD patterns of the sample that was prepared by mechanically milling NaH/Al with 4 mol % metallic Ti under Ar atmosphere for (a) 1 h, (b) 5 h, and (c) 10 h.

Clearly, the decreased particle size is favorable for kinetic improvement in both the dehydrogenation and hydrogenation processes.

(3) More homogeneous distribution and decreased size of the Ti-containing particles. As seen in Figure 8, a more homogeneous distribution of the Ti-containing particles in the NaH/Al matrix has been achieved after increasing the milling time from 1 to 10 h. The large Ti-containing particles with a diameter of several  $\mu\text{m}$  in the 1 h sample could no longer be observed in the sample milled for 10 h, but were substituted by many small particles with an average size of about 200–300 nm. According to the XRD results shown in Figure 6, most and/or a major part of the Ti-containing particles in the 1 h sample are metallic Ti. While in the 10 h sample, the observed particles should mainly consist of nanocrystalline  $\text{TiH}_2$ . Therefore, other than the mechanical smash, the brittleness of Ti hydride should also contribute to the disintegration and favorable dispersion of the Ti catalyst.

#### IV. Discussion

The nature of the active Ti species that catalyzes the reversible solid-state transformation of  $\text{NaAlH}_4$  has been a subject of great interest, speculation, and controversy. Several Ti-containing species, including Al–Ti alloy,<sup>16–22</sup>  $\text{Ti}^0$ ,<sup>2,5,17,20,23</sup> Ti hydride(s),<sup>26</sup> and Ti cation(s) with variable valance,<sup>24,25</sup> have been speculated as possible candidate of the catalytically active species. The first three fall into the surface catalysis, while the last speculation depicts a different “bulk” catalysis model in which the activation of  $\text{NaAlH}_4$  is associated with vacancy formation and lattice distortion arising upon lattice substitution of  $\text{Na}^+$  by  $\text{Ti}^{n+}$  ( $n = 2–4$ ).<sup>24</sup> In the hydrides doped with traditional Ti compounds, the direct and convincing identification of active species has been greatly hindered by the invisibility of Ti-containing species in conventional analytical techniques.

This situation was changed in the hydrides directly doped with metallic Ti. For the first time, it has been directly observed in XRD examination that mechanical milling of the host hydrides with metallic Ti leads to the formation of nanocrystalline Ti hydrides. Moreover, the direct doping of the hydrides with  $\text{TiH}_2$  was found to result in similar hydrogen storage performance to that arising upon doping the hydrides with metallic Ti. These results suggest that the in situ formed Ti hydrides act as catalytically active species. As a result, a surface catalysis mechanism should be involved in the reversible dehydrogenation/rehydrogenation of sodium aluminum hydride.

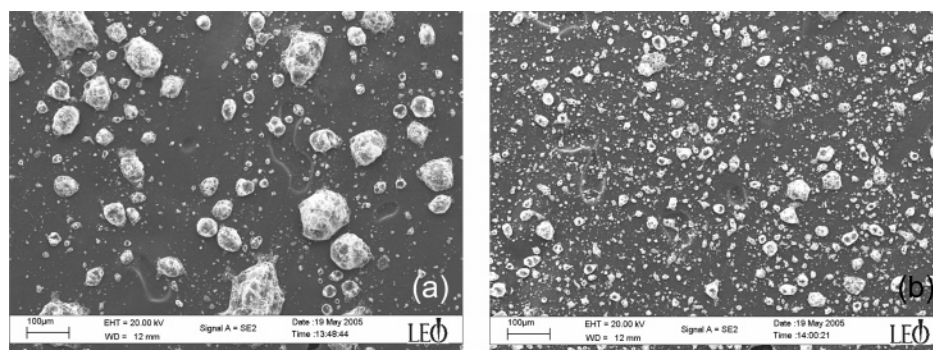


**Figure 7.** SEM morphology of NaH + Al + 4 mol % Ti mechanically milled under Ar atmosphere for (a) 1 h, (b) 10 h.

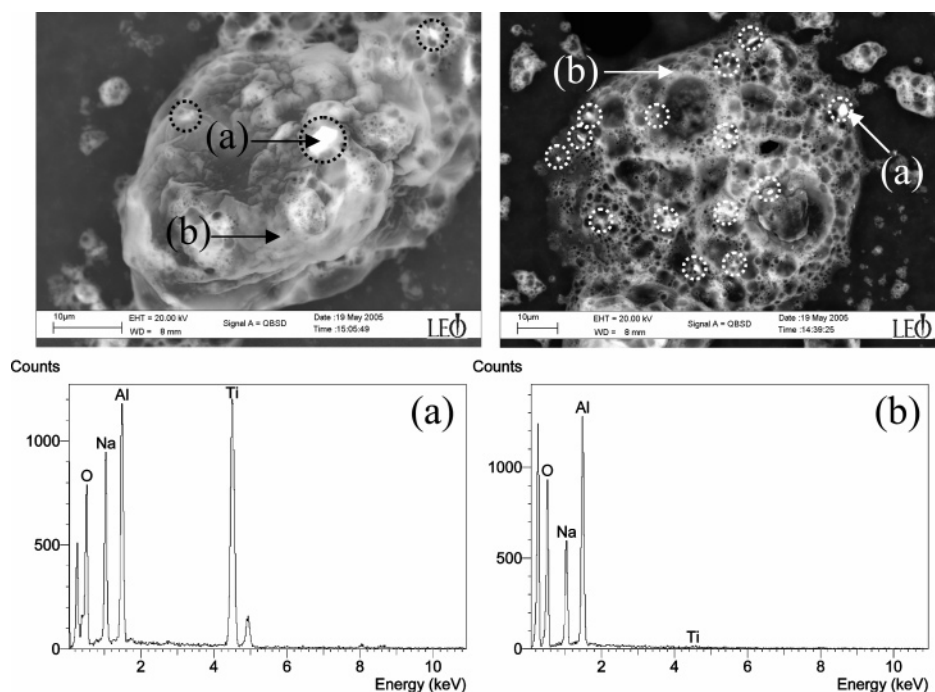


**Figure 8.** Backscattering electron (BSE) images of NaH + Al + 4 mol % Ti mechanically milled under Ar atmosphere for 1 h (top, left), 10 h (top, right), and the representative EDX results. The bright Ti-containing particles are encircled by dotted circles. It should be noted that, despite the special caution taken in sample transferring, a significant amount of oxygen contamination has been introduced into the samples.

On the rehydriding aspect, a general consideration of the catalysis mechanism may involve the promoted dissociation of hydrogen molecules into atoms. Actually, surface potential measurements have shown that hydrogen could be dissociatively adsorbed and form a unique state of atomic hydrogen adsorbate on the surface of TiH<sub>1.95</sub> film.<sup>38</sup> However, as is well-known, many other transition metals, e.g., Pt, Ni, Co, possess pronounced catalytic function to enhance the dissociation of molecular hydrogen. But meanwhile, it has been well-established that Ti species possess superiority in catalytic activity over other transition metal compounds.<sup>5,39</sup> Therefore, there should be a deeper mechanism involved in the rate-determining step in the hydrogenation of the NaH/Al mixture other than the dissociation of the H–H bond. Here, maybe a key hint is available from comparing the hydriding behaviors between metallic Al and the NaH/Al mixture. Metallic Al cannot be recharged via the gas–solid reaction, even after adding a Ti catalyst.<sup>40</sup> While the formation of hexahydride from the NaH/Al mixture and further reconstruction of tetrahydride is possible, it requires high H pressure and temperature conditions.<sup>5</sup> Therefore, NaH and Na<sub>3</sub>AlH<sub>6</sub> should play critical roles in the formation of the Al–H bond. With the presence of a Ti catalyst, the operation temperature and pressure conditions in the rehydriding process can be markedly reduced. This finding leads us to a hypothesis

that Ti hydride may soften Na<sup>+</sup>–H<sup>−</sup> and Na<sup>+</sup>–[AlH<sub>6</sub>]<sup>3−</sup> bonds because the destabilization of the ionic bonds of the hydrides should be a key step in facilitating the formation of the Al–H bond.

Currently, the underlying mechanism describing the observed catalytic enhancement of Ti hydrides on the dehydrogenation reactions of sodium aluminum hydrides is also being considered. One possibility is that TiH<sub>2</sub> destabilizes the Al–H bonds. The Al–H bond in tetra- and hexahydride and Ti–H bond in TiH<sub>2</sub> are polar covalent, where most of the electron charge is concentrated around H anions. When the two phases are close enough and adopt an appropriate spatial arrangement, local electrostatic attraction is expected to be developed between Ti<sup>n+</sup> ( $n < 2$ ) and the specific H<sup>−</sup> in [AlH<sub>4</sub>]<sup>−</sup>. Such an interaction may weaken and even result in the breaking of the Al–H bond if combined with a strengthened atomic vibration at elevated temperature. The released H may be temporarily trapped by a Ti cation, thus forming the intermediate transition state TiH<sub>*n*</sub> ( $n > 2$ ). The unstable hydride may release the extra H and transform back to TiH<sub>2</sub> rapidly.<sup>34</sup> The loss of one H in a [AlH<sub>4</sub>]<sup>−</sup> unit destroys the local electronic charge equilibrium and, as a result, may lead to the collapse of the NaAlH<sub>4</sub> lattice constructed of a Na<sup>+</sup> and [AlH<sub>4</sub>]<sup>−</sup> unit. Similar consideration may also be applied for the decomposition process of Na<sub>3</sub>AlH<sub>6</sub>.

For the metallic Ti-doped hydrides, the experimental evidence so far obtained suggests that the in situ formed Ti hydride acts as an active species. However, whether this finding can be safely generalized to the hydrides doped with traditional high-valance Ti compounds is still an open question. A main concern comes from the observation that the dehydrogenating/rehydrogenating kinetics of metallic Ti-doped hydrides was significantly inferior to that arising upon doping the hydrides with Ti(III) or Ti(IV) dopant precursors.<sup>27,28</sup> However, for heterogeneously catalyzed reactions, the practical catalytic effectiveness relies not only on the intrinsic activity of the catalyst, but also on the distribution state of the catalyst particles. In the case of the hydrides doped with Ti halides, it is believed and also experimentally shown that the high-valance  $Ti^{n+}$  is rapidly reduced to  $Ti^0$  via the highly exothermic reaction between the host hydrides and dopant precursors.<sup>2,5,17</sup> Thus formed,  $Ti^0$  has achieved an atomic-level dispersion in the hydride matrix that is much more favorable than that obtained by mechanically milling the hydrides with metallic Ti powder. As a result, the thermodynamically favorable formation of Ti hydride(s) during the doping and/or subsequent hydrogenating processes should be further kinetically facilitated. Clearly, if this process did occur, the formed Ti hydride phase(s) should also be highly dispersed in the hydride matrix. Such consideration may not only account for the observed prominent catalytic performance, but also the invisibility of Ti-containing species in XRD examination in the hydrides doped with Ti compounds. Therefore, one speculation is proposed here that various Ti-doped  $NaAlH_4$  samples that are prepared under different conditions share a common nature of active Ti species. What differs among these samples is the dispersion degree of the catalyst particles in the hydride matrix.

Finally, it should be noted that, while the in situ formed Ti hydride(s) has been identified as the active species, the possibility that other catalytically active Ti-containing species, e.g., Al–Ti alloy, were also formed during the milling and/or subsequent de-/hydrogenating cycles cannot yet be safely excluded. They may be present in an X-ray amorphous phase or in a small amount that falls below the detection limit of XRD technique. In this regard, further investigation on the chemical bonding state of Ti and specially designed experiments are currently underway to check this possibility.

## V. Conclusions

A systematic structure/property investigation on metallic Ti-doped  $NaAlH_4$  suggests that the nanocrystalline Ti hydride(s) in situ formed during the doping process acts as an active species to catalyze the reversible de-/hydrogenation of  $NaAlH_4$ . Titanium hydride may vary slightly in composition upon changing the starting material or milling atmosphere during the doping process or undergoing de-/hydrogenation cycles. The demonstrated nature of active Ti species clearly indicates that the reversible hydrogen storage of  $NaAlH_4$  at a moderate temperature range is governed by a heterogeneous surface catalysis mechanism. Advancement on the doping technology may lead to further improved hydrogen storage properties of  $NaAlH_4$ .

**Acknowledgment.** The financial support for this research from the Hundred Talents Project of the Chinese Academy of Sciences is gratefully acknowledged.

## References and Notes

- Schlapbach, L.; Züttel, A. *Nature* **2001**, *414*, 353.
- Bogdanović, B.; Schwickardi, M. *J. Alloys Compd.* **1997**, *253–254*, 1.
- Jensen, C. M.; Zidan, R.; Mariels, N.; Hee, A.; Hagen, C. *Int. J. Hydrogen Energy* **1999**, *24*, 461.
- Zidan, R. A.; Takara, S.; Hee, A. G.; Jensen, C. M. *J. Alloys Compd.* **1999**, *285*, 119.
- Bogdanović, B.; Brand, R. A.; Marjanović, A.; Schwickardi, M.; Tölle, J. *J. Alloys Compd.* **2000**, *302*, 36.
- Zaluska, A.; Zaluski, L.; Ström-Olsen, J. O. *J. Alloys Compd.* **2000**, *298*, 125.
- Balema, V. P.; Dennis, K. W.; Pecharsky, V. K. *Chem. Commun.* **2000**, 1665.
- Jensen, C. M.; Gross, K. J. *Appl. Phys. A* **2001**, *72*, 213.
- Bogdanović, B.; Schwickardi, M. *Appl. Phys. A* **2001**, *72*, 221.
- Gross, K. J.; Thomas, G. J.; Jensen, C. M. *J. Alloys Compd.* **2002**, *330–332*, 683.
- Sandrock, G.; Gross, K.; Thomas, G.; Jensen, C.; Meeker, D.; Takara, S. *J. Alloys Compd.* **2002**, *330–332*, 696.
- Sandrock, G.; Gross, K.; Thomas, G. *J. Alloys Compd.* **2002**, *339*, 299.
- Gross, K. J.; Majzoub, E. H.; Spangler, S. W. *J. Alloys Compd.* **2003**, *356–357*, 423.
- Fichtner, M.; Fuhr, O.; Kircher, O.; Rothe, J. *Nanotechnology* **2003**, *14*, 778.
- Bogdanović, B.; Felderhoff, M.; Kaskel, S.; Pommerin, A.; Schlichte, K.; Schüth, F. *Adv. Mater.* **2003**, *15*, 1012.
- Bogdanović, B.; Felderhoff, M.; Germann, M.; Härtel, M.; Pommerin, A.; Schüth, F.; Weidenthaler, C.; Zibrowius, B. *J. Alloys Compd.* **2003**, *350*, 246.
- Bellosta von Colbe, J. M.; Bogdanović, B.; Felderhoff, M.; Pommerin, A.; Schüth, F. *J. Alloys Compd.* **2003**, *370*, 104.
- Weidenthaler, C.; Pommerin, A.; Felderhoff, M.; Bogdanović, B.; Schüth, F. *Phys. Chem. Chem. Phys.* **2003**, *5*, 5149.
- Felderhoff, M.; Klementiev, K.; Grünert, W.; Spliethoff, B.; Bellosta von Colbe, J. M.; Bogdanović, B.; Härtel, M.; Pommerin, A.; Schüth, A.; Weidenthaler, C. *Phys. Chem. Chem. Phys.* **2004**, *6*, 4369.
- Schüth, F.; Bogdanović, B.; Felderhoff, M. *Chem. Commun.* **2004**, 2249.
- Brinks, H. W.; Jensen, C. M.; Srinivasan, S. S.; HauBack, B. C.; Blanchard, D.; Murphy, K. *J. Alloys Compd.* **2004**, *376*, 215.
- Graetz, J.; Reilly, J. J.; Johnson, J.; Ignatov, A. Yu.; Tyson, T. A. *Appl. Phys. Lett.* **2004**, *85*, 500.
- Lovvik, O. M.; Opalka, S. M. *Phys. Rev. B* **2005**, *71*, 054103.
- Sun, D.; Kiyobayashi, T.; Takeshita, H. T.; Kuriyama, N.; Jensen, C. M. *J. Alloys Compd.* **2002**, *337*, L8.
- Iniguez, J.; Yildirim, T.; Udovic, T. J.; Majzoub, E. H.; Sulic, M.; Jensen, C. M. *Phys. Rev. B* **2004**, *70*, 060101.
- Balema, V. P.; Balema, L. *Phys. Chem. Chem. Phys.* **2005**, *7*, 1310.
- Wang, P.; Jensen, C. M. *J. Alloys Compd.* **2004**, *379*, 99.
- Wang, P.; Jensen, C. M. *J. Phys. Chem. B* **2004**, *108*, 15827.
- Koch, C. C.; Whittenberger, J. D. *Intermetallics* **1996**, *4*, 339.
- Huot, J.; Liang, G.; Schulz, R. *Appl. Phys. A* **2001**, *72*, 187.
- Lü, L.; Lai, M. O. *Mechanical Alloying*; Kluwer: Boston, 1997.
- Soni, P. R. *Mechanical Alloying. Fundamentals and Applications*; Cambridge International Science: Cambridge, U.K., 2000.
- Wang, W. E. *J. Alloys Compd.* **1996**, *238*, 6.
- Barin, I. *Thermochemical Data of Pure Substances*; Wiley-VCH Verlag GmbH: Weinheim, 1988.
- Grochala, W.; Edwards, P. P. *Chem. Rev.* **2004**, *104*, 1283.
- The standard Gibbs free energy change of the reaction  $NaAlH_4 \rightarrow 1/3Na_3AlH_6 + 2/3Al + H_2$  is not available from the literature. It was estimated according to the formula:  $\Delta G_{dec}^\circ = \Delta H_{dec}^\circ - T\Delta S_{dec}^\circ$ . Here, the entropy change during the decomposition reaction is governed by the evolution of the molecular hydrogen. Thus,  $\Delta S_{dec}^\circ \approx S(H_2)^\circ = 130.7 \text{ J mol}^{-1} \text{ K}^{-1}$ .<sup>35</sup>
- Kang, M. H.; Wilkins, J. W. *Phys. Rev. B* **1990**, *41*, 10182.
- Nowicka, E.; Duś, R. *J. Alloys Compd.* **1997**, *253–254*, 506.
- Anton, D. L. *J. Alloys Compd.* **2003**, *356–357*, 400.
- Sandrock, G.; Reilly, J.; Graetz, J.; Zhou, W.-M.; Johnson, J.; Węgrzyn, J. *Appl. Phys. A* **2005**, *80*, 687.